ONLINE FIRST

This is a provisional PDF only. Copyedited and fully formatted versión will be made available at final publication

HISTOLOGY AND HISTOPATHOLOGY

ISSN: 0213-3911
e-ISSN: 1699-5848

In vitro and *in vivo* antineoplastic activities of solamargine in colorectal cancer through the suppression of PI3K/AKT pathway

Authors: Aihua Liu and Chunying Liu

DOI: 10.14670/HH-18-717
Article type: ORIGINAL ARTICLE
Accepted: 2024-01-31
Epub ahead of print: 2024-01-31

In vitro and *in vivo* antineoplastic activities of solamargine in colorectal cancer through the suppression of PI3K/AKT pathway

Running title: Solamargine as an anticancer monomer in CRC.

Aihua Liu, Chunying Liu

Department of Pathology, Liaoning University of Traditional Chinese Medicine, No.79 Chongshan Road, Huanggu District, Shenyang 110847, Liaoning Province, China

Correspondence to: Prof. Chunying Liu, Department of Pathology, Liaoning University of Traditional Chinese Medicine, No.79 Chongshan Road, Huanggu District, Shenyang 110847, Liaoning Province, China.

Tel: +86-024- 31207092; E-mail: chunying_liu99@163.com

Competing interests: The authors declare they have no competing interests.

Funding: Not applicable.

Acknowledgements: Not applicable.

Abstract

Purpose: Previous research has demonstrated the efficacy of SM in inhibiting tumor growth in various cancer types. The objective of this study was to examine the antineoplastic effects and molecular mechanisms of Solamargine (SM) in colorectal cancer. **Methods:** Colorectal cancer (CRC) cells were treated with different concentrations of SM to evaluate the anticancer concentration for further experimental measurements. Additionally, the antitumor efficacy of SM was assessed in a subcutaneously implanted tumor model of colorectal cancer. RNA-seq and bioinformatics analyses were employed to identify differentially expressed genes (DEGs) and elucidate the underlying molecular mechanisms in LoVo cells. Subsequently, the specific mechanism of SM-mediated anti-tumor activities was analyzed by protein expression methods. **Results:** The results of *in vitro* assays demonstrated that SM exhibits significant inhibitory effects on cell proliferation, clone formation, and invasion, while also promoting apoptosis in SW48 and LOVO cells. In a mouse xenograft tumor model, intragastric administration of SM at doses of 5 or 10 mg/kg effectively suppressed tumor volume and weight, and induced cell apoptosis *in vivo*. SM treatment also down-regulated PCNA and Cyclin E protein expression, contributing to the regulation of apoptosis. Further analysis using RNA-seq, bioinformatics, and experimental measurements revealed that SM treatment upregulates PTEN expression, while significantly reducing the phosphorylation levels of Akt and mTOR in LOVO cells. **Conclusion:** Our study provides further evidence to support the notion that SM primarily induces apoptosis in colorectal cancer cells through the inhibition of the PI3K/Akt signaling pathway. Additionally, our investigation demonstrated the favorable safety profile of SM in a mouse model of colorectal cancer, thereby suggesting its potential as a promising therapeutic approach for the management of CRC.

Keywords: colorectal cancer; solamargine; bioactive substance; PI3K/Akt; anti-tumor activity

Introduction

Colorectal cancer (CRC) estimated new cases and deaths are predicted to rank third (approximately accounting for 8%) in the United States in 2023 (Sung et al., 2021; Siegel et al., 2023). Global Cancer Statistics 2020 exhibited that there were an estimated 1,880,725 (accounting for 10.0%) new cases and 915,880 (accounting for 9.4%) cancer deaths of CRC, with ranking third of morbidity and second of mortality (Sung et al., 2021). The carcinogenesis of CRC is characterized with the turbulence of proliferation, apoptosis, differentiation and survival of intestinal epithelial cells, immune cells, stromal cells and commensal microbes (Chen et al., 2021; Sedlak et al., 2023). At present, the cancer treatment protocols for CRC mainly include radiotherapy, chemotherapy and surgical resection, while approximately 50% of recurrent events have been observed in patients with CRC (Boakye et al., 2018; Katona and Weiss, 2020). Unfortunately, patients with advanced CRC are less likely to be cured by surgery, and metastasis is the leading cause of death (Boakye et al., 2018). In addition, numerous side effects, such as decreased immune function, liver toxicity, and digestive disorders, are accompanied with radiotherapy and chemotherapy in CRC patients (Marin et al., 2012). Therefore, it is necessary to develop novel therapeutic strategies that can effectively cure CRC patients with the fewest adverse events.

Solamargine (SM), as a cholestane derivative of steroid alkaloids, is the main bioactive component of Solanum species such as Solanum nigrum (Sánchez-Mata et al., 2010; El-Hawary et al., 2016) and displays several therapeutic activities, such as anti-inflammatory effect (Zhao et al., 2022) and improvement of neurotoxicity (Zhang et al., 2020). The anti-

tumor effects of SM have been demonstrated in various types of cancer, including prostate cancer, lung cancer, liver cancer, and breast cancer. These effects are achieved through the inhibition of cancer cell growth, migration, invasion, and metastasis, as well as the promotion of apoptosis (Shiu et al., 2007; Ding et al., 2012; Xiang et al., 2016; Kalalinia and Karimi-Sani, 2017; Furtado et al., 2022; Yin et al., 2022). For example, SM has been shown to inhibit cell growth in castration-resistant prostate cancer cells by activating the MAPK signaling pathway and reducing the expression of the downstream protein MUC1 (Xiang et al., 2016). Additionally, SM has been found to enhance cisplatin sensitivity in breast cancer cells and induce G2/M phase cell cycle arrest in human hepatoma SMMC-7721 cells (Shiu et al., 2007; Ding et al., 2012). Recently, it has been demonstrated that SM induces apoptosis and autophagy in hepatocellular carcinoma cells through the inhibition of the LIF/miR-192-5p/CYR61/Akt signaling pathways and the induction of an immunostimulatory tumor microenvironment (Yin et al., 2022). In a mouse model of melanoma, the subcutaneous administration of SM resulted in a reduction in tumor size and frequency of mitoses in tumor tissue, indicating a decrease in cell proliferation (Furtado et al., 2022). These findings suggest that SM has the potential to inhibit proliferation and promote apoptosis in various cancer cells. However, the effect of SM on colorectal cancer cells remains uncertain, and the underlying mechanisms of SM have yet to be elucidated.

The objective of our study was to investigate the antineoplastic effects of SM on colorectal cancer both *in vivo* and *in vitro*. Additionally, we utilized RNA-seq and bioinformatics techniques to analyze the differential gene expression in LoVo cells pre- and post-treatment with SM, aiming to elucidate the underlying molecular mechanism of SM in treating colorectal cancer. Our findings demonstrated that SM primarily induced apoptosis in colorectal cancer cells by inhibiting the phosphatidylinositol 3-kinase (PI3K)/protein kinase

B (AKT) signaling pathway. Furthermore, SM exhibited promising safety profiles in a mouse model of CRC.

Materials and methods

Reagents and antibodies. The main reagents and antibodies are listed as follows: RPMI1640 medium (Gibco, USA), fetal bovine serum (FBS; Hyclone, USA), MTT (Sigma, USA), SM (Sigma, USA), Annexin V-FITC/PI apoptosis detection kit (BD Biosciences, USA), Ki67 (Cat. no: RPN202; GE, USA), TUNEL (Beyotime, China), anti-phosphatase and tensin homologue deleted on chromosome 10 (anti-PTEN; Cat. no: #9552; CTS, USA), AKT (Cat. no: #9272, CTS, USA), p-AKT (Cat. no: #4058; CTS, USA), p-mTOR (Cat. no: #2971; CTS, USA), β-actin (Cat. no: #4967; CTS, USA), PCNA (Cat. no: #13110; CTS, USA), cyclin E (Cat. no: #4132; CTS, USA), cleaved caspase 7 (Cat. no: #9491; CTS, USA), caspase 7 (Cat. no: #9492; CTS, USA), cleaved caspase 9 (Cat. no: #9507; CTS, USA), caspase 9 (Cat. no: #9502; CTS, USA), Bcl-2 (Cat. no: #3498; CTS, USA) and BAX (Cat. no: #2772; CTS, USA).

Cell culture. SW48 and LoVo were cultured in RPMI1640 medium, supplemented with 10% FBS and 1% penicillin/streptomycin (Gibco; Thermo Fisher Scientific, Inc.). All cells were cultured at 37°C and 5% CO2. After incubation with SM (0, 2, 4, 8, 16, 32 μM) for different times, SW48 and LoVo cells were used for molecular biology experiments. SM was dissolved in dimethyl sulfoxide (DMSO). Insulin-like growth factor-1 (IGF-1; 100 ng/mL; Gibco) as a potential PI3K/AKT agonist was used to activate the PI3K/AKT signaling pathway in LoVo cells.

***In vitro* measurements of MTT, colony formation, flow cytometry, transwell and wound scratch assays.** The above-mentioned assays were performed as we described previously (Shen et al., 2020; Sun et al., 2021).

Animal model. BALB/c nude mice were acquired from the Beijing Vital River Laboratory Animal Technology (Beijing, China). Following the subcutaneous injection of LoVo cells (2×10^6 cells) into the BALB/c nude mice, intragastric administration of SM (5 mg/kg/day or 10 mg/kg/day) was conducted from day 10 to day 24. Subsequently, the body weight of the nude mice, tumor volume and weight, and the IHC staining of Ki67 and TUNEL were employed to assess the *in vivo* anti-proliferative and pro-apoptotic properties of SM.

Immunohistochemical (IHC) and immunofluorescence (IF) staining. The operation procedures of IHC and IF staining were performed as described previously (Liu et al., 2016; Ren et al., 2019). Ki67 (Cat. no: RPN202; GE, USA; dilution: 1: 100) and TUNEL kit (Beyotime, China) were used to evaluate Ki67 protein expression and cell apoptosis.

RNA sequencing (RNA-seq) and bioinformatics analysis. In order to investigate the signaling pathways involved in SM-induced cell death in CRC cells, RNA-seq analysis was conducted using Majorbio (Shanghai, China) to identify DEGs in LoVo cells treated with SM at a concentration of 32μM for 48 hours. The DEGs were then subjected to Gene Ontology (GO) and Kyoto Encyclopedia of Genes and Genomes (KEGG) pathway enrichment analysis using the DAVID database.

RNA extraction and reverse transcription-quantitative PCR (RT-qPCR). RNA extraction and RT-qPCR were conducted according to the methods described in previous studies (Shen et al., 2020; Sun et al., 2021) with the primers as follows: forward primer, 5'-TGGATTCGACTTAGACTTGACCT-3' and reverse primer, 5'-GGTGGGTTATGGTCTTCAAAAGG-3' for PTEN; forward primer, 5'-CCCGAGAGGTCTTTTTCCGAG-3' and reverse primer, 5'-CCAGCCCATGATGGTTCTGAT-3' for BAX; forward primer, 5'-GCAGGCGTCGAAGAGTACG-3' and reverse primer, 5'-CGGACTGCGATTGCAGAAGA-3' for VHL; forward primer, 5'-GGTTCGGACATCACAAGTAGTAG-3' and reverse primer, 5'-GGTGTGCCGATTCCTTTCTCT-3' for ZHX2; forward primer, 5'-ACTCACCTCTTCAGAACGAATTG-3' and reverse primer, 5'-CCATCTTTGGAAGGTTCAGGTTG-3' for IL6; forward primer, 5'-TGGAGCTGCCTACGTGTATG-3' and reverse primer, 5'-TTCGATGAGTAGAAAGCAGTGC-3' for IL5; forward primer, 5'-CTGCTGCTACTACTTACAAGGTC-3' and reverse primer, 5'-GCAGGGCAGATAGGCATTCT-3' for TIM3; forward primer, 5'-GGTGATGGGGAACCTTGAGAT-3' and reverse primer, 5'-CTGTCACTTCTCGAATCCACTG-3' for HER3; forward primer, 5'-TAAGTTCTGAGTGTGACCGAGA-3' and reverse primer, 5'-GCTCTGTCTGTAGGGAGGTAGG-3' for BIM; forward primer, 5'-GGTGGGGTCATGTGTGTGG-3' and reverse primer, 5'-CGGTTCAGGTACTCAGTCATCC-3' for BCL2; forward primer, 5'-ACATCGCTCAGACACCATG-3' and reverse primer, 5'-TGTAGTTGAGGTCAATGAAGGG-3' for GAPDH.

Western blot. The detailed procedures of western blot were performed as we described previously (Shen et al., 2020; Sun et al., 2021).

Statistical analysis. The data were reported as the mean ± standard deviation. Statistical analysis was conducted using SPSS (Version 19.0). Two-group differences were analyzed using either the student's t-test or the nonparametric Mann-Whitney test. Inter-group differences were assessed through One-Way ANOVA. A p-value below 0.05 was considered indicative of statistical significance.

Results

SM exhibited the potent antineoplastic activities *in vitro*. To evaluate the antineoplastic activities of SM in CRC cell lines, SW48 and LoVo, the MTT, clone formation, flow cytometry, transwell and wound scratch assays were implemented to determine the effect of SM on SW48 and LoVo cell proliferation, apoptosis, invasion and migration *in vitro*. After SW48 and LoVo cells exposure to SM with the concentration range from 0 μM to 32 μM, MTT assay suggested that SM significantly suppresses SW48 and LoVo cell proliferation in a dose-dependent and time-dependent manner (**Fig. 1A**), and the inhibition ratio was 80.2% and 78.7 in SW48 and LoVo cells, respectively, after incubation with SM with the concentration of 32 μM (**Fig. 1A**). After SW48 and LoVo cells treatment with SM (0-32μM) for 72h, there was a significant decrease in the number of cell clones in a dose-dependent manner (**Fig. 1B**). Cell clones were reduced approximately 97% in both SW48 and LoVo3 cells, exposed to SM with the concentration of 32 μM (**Fig. 1B**). As shown in **Figure 1C**, SM significantly enhanced the proportion of apoptotic cells in a dose-dependent manner compared with the control group. We also performed invasion and migration experiments.

Transwell (**Fig. 1D**) and wound scratch assays (**Fig. 1E**) found that SW48 and LoVo cell invasion and migration abilities were significantly hindered in the dose-dependent manner with the presence of SM exposure. Our findings indicated that SM showed the potent antineoplastic activities *in vitro*.

SM impeded LoVo cell growth *in vivo*. The effect of SM on LoVo cell growth was also investigated in a nude mice xenograft tumor model. After BALB/c nude mice injected with LoVo cells (2×10^6 cells) subcutaneously, mice were intragastrically administrated with SM (5 mg/kg/day or 10 mg/kg/day) from day 10 to day 24. As shown in **Figure 2A**, the body weight had no obvious difference in transplanted tumor mice with or without SM treatment, suggesting that SM has no apparent toxicity *in vivo*. Subsequently, tumor volume (**Fig. 2B**) and tumor weight (**Fig. 2C**) were markedly delayed by the treatment of SM in a concentration of 5 mg/kg or 10 mg/kg. By IHC and TUNEL assay (**Fig. 2D and 2E**), a significant decrease in Ki67-positive cells accompanied with an increase in TUNEL-positive cell was presented in transplanted tumor mice with SM treatment.

SM mediated multiple signal pathways to suppress LoVo cell growth. To explore signaling pathways underlying SM-mediated CRC cell death, RNA-seq was implemented to filtrate DEGs in SM-treated LoVo cells. As shown in **Figure 3A**, a total of 538 DEGs, including 117 down-regulated and 421 up-regulated genes, were observed in SM-treated LoVo cells compared with control group. The top 10 DEGs were listed as follows: BCL2, TIM3, VHL, IL6, BAX, PTEN, IL-5, ZHX2, HER3 and Bim (**Fig. 3B**). The expression levels of the top 10 DEGs were also verified by RT-qPCR, which achieved consistent findings with RNA-seq (**Fig. 3C**). SM-mediated signaling pathways were enriched by KEGG analysis. Our results demonstrated that multiple pathways, such as PI3K/AKT, TGF-β/WNT, EGFR and

apoptosis signaling, were involved in SM-mediated CRC cell death.

SM activates PTEN and inhibits PI3K/AKT signaling to induce CRC cell death. In *in vitro* experimental measurements, a significant increase in PTEN protein level and decrease in p-AKT and p-mTOR appeared in SM-treated LoVo cells (**Fig. 4A**). Immunofluorescent (IF) staining showed that PTEN fluorescence intensity was markedly elevated in SM-treated LoVo cells compared with the control group (**Fig. 4B**). Consistent with *in vitro* findings, activation of PTEN and inhibition of PI3K/AKT signaling were represented in tumor tissues of transplanted tumor mice (**Fig. 4C**). IHC staining indicated that integral optical density (IOD) of p-AKT and p-mTOR were dramatically decreased, while IOD of PTEN was augmented in tumor tissues of transplanted tumor mice (**Fig. 4D**).

Numerous pieces of evidence substantiated that IGF-1 is an agonist to activate PI3K/AKT signaling in cancer progression (Wang et al., 2017; Zheng et al., 2020). In *in vitro* rescue experiments, we investigated whether IGF-1 would rescue SM-induced inhibition of cell proliferation, invasion and migration of LoVo cells. Our results indicated that SM-induced inhibition of clone formation (**Fig. 5A**), invasion (**Fig. 5B**) and migration (**Fig. 5C**) of LoVo cells were reversed by the co-incubation with IGF-1.

PCNA and Cyclin E were the key factors to regulate DNA replication and cell cycle (Strzalka and Ziemienowicz, 2011; Zeng et al., 2023). In our study, SM treatment inhibited the protein expression of PCNA and Cyclin E *in vitro* (**Fig. 6A**) and *in vivo* (**Fig. 6B**). Furthermore, the induction of pro-apoptotic proteins, namely cleaved-caspase-7, cleaved-caspase-9, and BAX, along with the suppression of the anti-apoptotic protein Bcl-2, was observed in LoVo cells treated with SM both *in vitro* (**Fig. 6C**) and *in vivo* (**Fig. 6D**). We also found that IF staining

and IHC staining IOD of BAX was augmented in LoVo cells (**Fig. 6E**) and tumor tissues (**Fig. 6F**) of transplanted tumor mice with SM treatment.

Discussion

SM has been corroborated to possess multiple antitumor properties via different signaling pathways (Shiu et al., 2008; Chen et al., 2015; Wu et al., 2020; Han et al., 2022; Yin et al., 2022). For example, the antineoplastic activities of SM in HCC reflected that inhibition of oncogenic factor, leukemia inhibitory factor, by SM treatment improves tumor microenvironment, including elevation of the proportion of CD8+ T cells and M1/M2 macrophages, and promotes apoptosis and autophagy (Yin et al., 2022). In human lung cancer cells, phosphorylation of Akt and NF-κB/p65 was impeded by SM administration to inhibit cell proliferation (Chen et al., 2015). In human epidermal growth factor receptor-2 (HER2) overexpressed breast cancer cells, SM down-regulated HER2 receptors on the cell membrane to enhance the sensitivity of chemotherapeutic agents (Shiu et al., 2008). In addition, the chemosensitization of SM was also found in cisplatin-resistant NSCLC organoids by suppressing the hedgehog pathway (Han et al., 2022). According to Wu et al (Wu et al., 2020), SM inhibits long non-coding RNA colon cancer-associated transcript1-mediated down-regulation of specific protein 1 to prevent human nasopharyngeal carcinoma cell growth. Lee and colleagues (Lee et al., 2004) found that the growth inhibition rate of SM was 1.3%, 28.9%, 71.8% or 82.0% with four concentrations each (0.1, 1, 10, or 100 μg/mL) in human colon HT29 cancer cells. However, the molecular mechanisms underlying SM-induced CRC cell growth inhibition and apoptosis are still unclear.

In our study, SM significantly suppressed SW48 and LoVo cell proliferation, colony formation, migration and invasion, and facilitated cell apoptosis in a dose-dependent manner

in vitro. In *in vivo* experiments nude-mouse transplanted tumor model and IHC staining, SM suppressed LoVo cell growth *in vivo* by inhibiting cell proliferation and inducing cell apoptosis, reflecting a significant decrease in Ki67-positive cells and an increase in TUNEL-positive cells in tumor tissues. Importantly, RNA-seq, bioinformatics and experimental evidence revealed that PTEN, PI3K/AKT and caspase9/7 were mainly mediators of SM-induced antineoplastic properties in CRC.

PI3K/AKT is a pivotal intracellular lipid kinase signaling pathway that is implicated in regulation of cell growth in various cancer types (He et al., 2021; Yu et al., 2022). Moreover, overactivation of PI3K/AKT plays a crucial role in the processes of 5-fluorouracil resistance (Dong et al., 2022), vasculogenic mimicry (Liu et al., 2022), metastasis (Jiang et al., 2021), tumor stemness (Mangiapane et al., 2022), macrophage M2 polarization (Zhao et al., 2020) in CRC. Herein, we also found that inactivation of PI3K/AKT hampers the malignant phenotypes of CRC cells, while PI3K/AKT agonist, IGF-1, could reverse SM-induced inhibition of clone formation, invasion and migration of LoVo cells, suggesting that PI3K/AKT may be a potential therapeutic target of SM in CRC.

Previous studies exhibited that the PIK3 gene is frequently mutated in CRC tumours with approximately 10%-20% samples (Prossomariti et al., 2020; Zygulska and Pierzchalski, 2022), and regulates downstream pathways of EGFR alongside with KRAS (Zygulska and Pierzchalski, 2022). Moreover, the initiation of PI3K signaling pathway can be inhibited by PTEN, which is an important tumor suppressor in CRC to counteract PI3K function (Molinari and Frattini, 2013; Chong et al., 2022; Zygulska and Pierzchalski, 2022). In our study, over-activation of PTEN was synchronized with the devitalization of p-AKT and p-mTOR in CRC cells after treatment with SM. Our findings suggested that SM is able to inhibit

PI3K/AKT/mTOR axis via the activation of PTEN in CRC.

Cyclin E mediates G1-S transition and contributes to tumor cell proliferation (Fukuse et al., 2000). PCNA also functions as cell cycle and proliferation related protein, and correlates with Cyclin E in inflammatory bowel disease-related dysplasia-carcinoma (Ioachim et al., 2004). Reduction of PCNA and Cyclin E protein expression is accompanied with the inhibition of cell proliferation and metastasis in CRC (Dai et al., 2014; Lin et al., 2018). Our results showed that SM treatment down-regulated PCNA and Cyclin E protein expression, with reduced cell proliferation and colony formation. These findings rationalize an important signaling pathway of SM-mediated CRC treatment.

In the mitochondrial apoptotic pathway, a multimeric Apaf-1/cytochrome c complex recruits and activates caspase 9 to cleave and promote the downstream caspases, including caspase 7 (Budihardjo et al., 1999). Up-regulation of cleaved-caspase 7 and cleaved-caspase 9 regulate cell cycle control and apoptosis in CRC cells (Wen et al., 2019). Similarly, SM treatment activates caspase 9/7 axis and BAX, with a corresponding elevation of the proportion of apoptotic cells in *in vivo* and *in vitro* CRC cells.

Conclusions

The findings of our study indicate that the administration of SM effectively inhibits the malignant characteristics of CRC cells both *in vitro* and *in vivo*. This inhibition is achieved through the suppression of the PI3K/AKT signaling pathway, which is a key pathway involved in cell growth and survival. Additionally, SM administration leads to the inhibition of cell cycle regulators, namely PCNA and Cyclin E, and the activation of the caspase 9/7 axis, resulting in the control of cell proliferation and induction of apoptosis. These results

provide substantial evidence for the potent antineoplastic properties of SM in CRC, acting through multiple signaling pathways. Therefore, SM holds promise as a highly effective small-molecule drug for the treatment of CRC.

Declarations:

Authors' contributions: A.L. and C.L. were responsible for study design. A.L. and C.L. were responsible for literature research, data acquisition, data analysis. A.L. and C.L. were responsible for manuscript preparation, manuscript editing, manuscript review, and cell and animal experiments. Final version to be published was approved by A.L. and C.L.

Ethical approval: Our study was approved by the Ethics Committee of the Liaoning University of Traditional Chinese Medicine (Shenyang, China).

References

Boakye D., Rillmann B., Walter V., Jansen L., Hoffmeister M. and Brenner H. (2018). Impact of comorbidity and frailty on prognosis in colorectal cancer patients: A systematic review and meta-analysis. Cancer. Treat. Rev. 64, 30-39.

Budihardjo I., Oliver H., Lutter M., Luo X. and Wang X. (1999). Biochemical pathways of caspase activation during apoptosis. Annu. Rev. Cell. Dev. Biol. 15, 269-290.

Chen Y., Tang Q., Wu J., Zheng F., Yang L. and Hann S.S. (2015). Inactivation of Pi3-K/Akt and reduction of SP1 and p65 expression increase the effect of solamargine on suppressing EP4 expression in human lung cancer cells. J. Exp. Clin. Cancer. Res. 34, 154.

Chen B., Scurrah C.R., McKinley E.T., Simmons A.J., Ramirez-Solano M.A., Zhu X., Markham N.O., Heiser C.N., Vega P.N., Rolong A., Kim H., Sheng Q., Drewes J.L., Zhou Y., Southard-Smith A.N., Xu Y., Ro J., Jones A.L., Revetta F., Berry L.D., Niitsu

H., Islam M., Pelka K., Hofree M., Chen J.H., Sarkizova S., Ng K., Giannakis M., Boland G.M., Aguirre A.J., Anderson A.C., Rozenblatt-Rosen O., Regev A., Hacohen N., Kawasaki K., Sato T., Goettel J.A., Grady W.M., Zheng W., Washington M.K., Cai Q., Sears C.L., Goldenring J.R., Franklin J.L., Su T., Huh W.J., Vandekar S., Roland J.T., Liu Q., Coffey R.J., Shrubsole M.J. and Lau K.S. (2021). Differential pre-malignant programs and microenvironment chart distinct paths to malignancy in human colorectal polyps. Cell 184, 6262-6280.

Chong X., Chen J., Zheng N., Zhou Z., Hai Y., Chen S., Zhang Y., Yu Q., Yu S., Chen Z., Bao W., Quan M., Chen Z.S., Zhan Y. and Gao Y. (2022). PIK3CA mutations-mediated downregulation of circLHFPL2 inhibits colorectal cancer progression via upregulating PTEN. Mol. Cancer. 21, 118.

Dai Y., Wilson G., Huang B., Peng M., Teng G., Zhang D., Zhang R., Ebert M.P., Chen J., Wong B.C., Chan K.W., George J. and Qiao L. (2014). Silencing of Jagged1 inhibits cell growth and invasion in colorectal cancer. Cell. Death. Dis. 5, e1170.

Ding X., Zhu F.S., Li M. and Gao S.G. (2012). Induction of apoptosis in human hepatoma SMMC-7721 cells by solamargine from Solanum nigrum L. J. Ethnopharmacol. 139, 599-604.

Dong S., Liang S., Cheng Z., Zhang X., Luo L., Li L., Zhang W., Li S., Xu Q., Zhong M., Zhu J., Zhang G. and Hu S. (2022). ROS/PI3K/Akt and wnt/β-catenin signalings activate HIF-1α-induced metabolic reprogramming to impart 5-fluorouracil resistance in colorectal cancer. J. Exp. Clin. Cancer. Res. 41, 15.

El-Hawary S.S., Mohammed R., AbouZid S.F., Bakeer W., Ebel R., Sayed A.M. and Rateb M.E. (2016). Solamargine production by a fungal endophyte of Solanum nigrum. J. Appl. Microbiol. 120, 900-911.

Fukuse T., Hirata T., Naiki H., Hitomi S. and Wada H. (2000). Prognostic significance of

cyclin E overexpression in resected non-small cell lung cancer. Cancer Res. 60, 242-244.

Furtado R.A., Ozelin S.D., Ferreira N.H., Miura B.A., Almeida Junior S., Magalhães G.M., Nassar E.J., Miranda M.A., Bastos J.K. and Tavares D.C. (2022). Antitumor activity of solamargine in mouse melanoma model: Relevance to clinical safety. J. Toxicol. Environ. Health. A. 85, 131-142.

Han Y., Shi J., Xu Z., Zhang Y., Cao X., Yu J., Li J. and Xu S. (2022). Identification of solamargine as a cisplatin sensitizer through phenotypical screening in cisplatin-resistant NSCLC organoids. Front. Pharmacol. 13, 802168.

He Y., Sun M.M., Zhang G.G., Yang J., Chen K.S., Xu W.W. and Li B. (2021). Targeting PI3K/Akt signal transduction for cancer therapy. Signal. Transduct. Target. Ther. 6, 425.

Ioachim E.E., Katsanos K.H., Michael M.C., Tsianos E.V. and Agnantis N.J. (2004). Immunohistochemical expression of cyclin D1, cyclin E, p21/waf1 and p27/kip1 in inflammatory bowel disease: Correlation with other cell-cycle-related proteins (Rb, p53, ki-67 and PCNA) and clinicopathological features. Int. J. Colorectal. Dis. 19, 325-333.

Jiang T., Wang H., Liu L., Song H., Zhang Y., Wang J., Liu L., Xu T., Fan R., Xu Y., Wang S., Shi L., Zheng L., Wang R. and Song J. (2021). CircIL4R activates the PI3K/AKT signaling pathway via the miR-761/TRIM29/PHLPP1 axis and promotes proliferation and metastasis in colorectal cancer. Mol. Cancer. 20, 167.

Kalalinia F. and Karimi-Sani I. (2017). Anticancer properties of solamargine: A systematic review. Phytother. Res. 31, 858-870.

Katona B.W. and Weiss J.M. (2020). Chemoprevention of colorectal cancer. Gastroenterology. 158, 368-388.

Lee K.R., Kozukue N., Han J.S., Park J.H., Chang E.Y., Baek E.J., Chang J.S. and Friedman M. (2004). Glycoalkaloids and metabolites inhibit the growth of human colon (HT29) and liver (HepG2) cancer cells. J. Agric. Food. Chem. 52, 2832-2839.

Lin K., Jiang H., Zhang L.L., Jiang Y., Yang Y.X., Qiu G.D., She Y.Q., Zheng J.T., Chen C., Fang L. and Zhang S.Y. (2018). Down-regulated lncRNA-HOTAIR suppressed colorectal cancer cell proliferation, invasion, and migration by mediating p21. Dig. Dis. Sci. 63, 2320-2331.

Liu Z., Dou C., Yao B., Xu M., Ding L., Wang Y., Jia Y., Li Q., Zhang H., Tu K., Song T. and Liu Q. (2016). Ftx non coding RNA-derived miR-545 promotes cell proliferation by targeting RIG-I in hepatocellular carcinoma. Oncotarget 7, 25350-25365.

Liu X., He H., Zhang F., Hu X., Bi F., Li K., Yu H., Zhao Y., Teng X., Li J., Wang L., Zhang Y. and Wu Q. (2022). m6A methylated EphA2 and VEGFA through IGF2BP2/3 regulation promotes vasculogenic mimicry in colorectal cancer via PI3K/AKT and ERK1/2 signaling. Cell. Death. Dis. 13, 483.

Mangiapane L.R., Nicotra A., Turdo A., Beyes S., Fagnocchi L., Fiori M.E., Gaggianesi M., Bianca P., Di Franco S., Sardina D.S., Veschi V. and Signore M. (2022). Pi3K-driven HER2 expression is a potential therapeutic target in colorectal cancer stem cells. Gut 71, 119-128.

Marin J.J., Sanchez de Medina F., Castaño B., Bujanda L., Romero M.R., Martinez-Augustin O., Moral-Avila R.D. and Briz O. (2012). Chemoprevention, chemotherapy, and chemoresistance in colorectal cancer. Drug. Metab. Rev. 44, 148-172.

Molinari F. and Frattini M. (2013). Functions and regulation of the PTEN gene in colorectal cancer. Front. Oncol. 3, 326.

Prossomariti A., Piazzi G., Alquati C. and Ricciardiello L. (2020). Are Wnt/β-Catenin and PI3K/AKT/mTORC1 distinct pathways in colorectal cancer? Cell. Mol. Gastroenterol.

Hepatol. 10, 491-506.

Ren L., Chen H., Song J., Chen X., Lin C., Zhang X., Hou N., Pan J., Zhou Z., Wang L., Huang D., Yang J., Liang Y., Li J., Huang H. and Jiang L. (2019). MiR-454-3p-mediated wnt/β-catenin signaling antagonists suppression promotes breast cancer metastasis. Theranostics. 9, 449-465.

Sánchez-Mata M.C., Yokoyama W.E., Hong Y.J. and Prohens J. (2010). Alpha-solasonine and alpha-solamargine contents of gboma (Solanum macrocarpon L.) and scarlet (Solanum aethiopicum L.) eggplants. J. Agric. Food. Chem. 58, 5502-5508.

Sedlak J.C., Yilmaz Ö H. and Roper J. (2023). Metabolism and colorectal cancer. Annu. Rev. Pathol. 18, 467-492.

Shen D., Wang Y., Niu H. and Liu C. (2020). Gambogenic acid exerts anticancer effects in cisplatin-resistant non-small cell lung cancer cells. Mol. Med. Rep. 21, 1267-1275.

Shiu L.Y., Chang L.C., Liang C.H., Huang Y.S., Sheu H.M. and Kuo K.W. (2007). Solamargine induces apoptosis and sensitizes breast cancer cells to cisplatin. Food. Chem. Toxicol. 45, 2155-2164.

Shiu L.Y., Liang C.H., Huang Y.S., Sheu H.M. and Kuo K.W. (2008). Downregulation of HER2/neu receptor by solamargine enhances anticancer drug-mediated cytotoxicity in breast cancer cells with high-expressing HER2/neu. Cell. Biol. Toxicol. 24, 1-10.

Siegel R.L., Miller K.D., Wagle N.S. and Jemal A. (2023). Cancer statistics, 2023. CA. Cancer. J. Clin. 73, 17-48.

Strzalka W. and Ziemienowicz A. (2011). Proliferating cell nuclear antigen (PCNA): A key factor in DNA replication and cell cycle regulation. Ann. Bot. 107, 1127-1140.

Sun Y., Liu W., Zhao Q., Zhang R., Wang J., Pan P., Shang H., Liu C. and Wang C. (2021). Down-regulating the expression of miRNA-21 inhibits the glucose metabolism of A549/DDP cells and promotes cell death through the PI3K/AKT/mTOR/HIF-1α

pathway. Front. Oncol. 11, 653596.

Sung H., Ferlay J., Siegel R.L., Laversanne M., Soerjomataram I., Jemal A. and Bray F. (2021). Global cancer statistics 2020: GLOBOCAN estimates of incidence and mortality worldwide for 36 cancers in 185 countries. CA. Cancer. J. Clin. 71, 209-249.

Wang G., Lu M., Yao Y., Wang J. and Li J. (2017). Esculetin exerts antitumor effect on human gastric cancer cells through IGF-1/PI3K/Akt signaling pathway. Eur. J. Pharmacol. 814, 207-215.

Wen J., Liu X., Qi Y., Niu F., Niu Z., Geng W., Zou Z., Huang R., Wang J. and Zou H. (2019). BMP3 suppresses colon tumorigenesis via ActRIIB/SMAD2-dependent and TAK1/JNK signaling pathways. J. Exp. Clin. Cancer. Res. 38, 428.

Wu J., Tang X., Ma C., Shi Y., Wu W. and Hann S.S. (2020). The regulation and interaction of colon cancer-associated transcript-1 and mir7-5p contribute to the inhibition of SP1 expression by solamargine in human nasopharyngeal carcinoma cells. Phytother. Res. 34, 201-213.

Xiang S., Zhang Q., Tang Q., Zheng F., Wu J., Yang L. and Hann S.S. (2016). Activation of AMPKα mediates additive effects of solamargine and metformin on suppressing MUC1 expression in castration-resistant prostate cancer cells. Sci. Rep. 6, 36721.

Yin S., Jin W., Qiu Y., Fu L., Wang T. and Yu H. (2022). Solamargine induces hepatocellular carcinoma cell apoptosis and autophagy via inhibiting LIF/miR-192-5p/CYR61/Akt signaling pathways and eliciting immunostimulatory tumor microenvironment. J. Hematol. Oncol. 15, 32.

Yu L., Wei J. and Liu P. (2022). Attacking the PI3K/Akt/mTOR signaling pathway for targeted therapeutic treatment in human cancer. Semin. Cancer. Biol. 85, 69-94.

Zeng J., Hills S.A., Ozono E. and Diffley J.F.X. (2023). Cyclin E-induced replicative stress

drives p53-dependent whole-genome duplication. Cell. 186, 528-542.

Zhang H., Tian F., Jiang P., Qian S., Dai X., Ma B., Wang M., Dai H., Sha X., Yang Z., Zhu X. and Sun X. (2020). Solasonine suppresses the proliferation of acute monocytic leukemia through the activation of the AMPK/FOXO3A axis. Front. Oncol. 10, 614067.

Zhao S., Mi Y., Guan B., Zheng B., Wei P., Gu Y., Zhang Z., Cai S., Xu Y., Li X., He X., Zhong X., Li G., Chen Z. and Li D. (2020). Tumor-derived exosomal miR-934 induces macrophage M2 polarization to promote liver metastasis of colorectal cancer. J. Hematol. Oncol. 13, 156.

Zhao J., Dan Y., Liu Z., Wang Q., Jiang M., Zhang C., Sheu H.M., Lin C.S. and Xiang L. (2022). Solamargine alleviated UVB-induced inflammation and melanogenesis in human keratinocytes and melanocytes *via* the p38 MAPK signaling pathway, a promising agent for post-inflammatory hyperpigmentation. Front. Med. (Lausanne) 9, 812653.

Zheng Y., Wu C., Yang J., Zhao Y., Jia H., Xue M., Xu D., Yang F., Fu D., Wang C., Hu B., Zhang Z., Li T., Yan S., Wang X., Nelson P.J., Bruns C., Qin L. and Dong Q. (2020). Insulin-like growth factor 1-induced enolase 2 deacetylation by HDAC3 promotes metastasis of pancreatic cancer. Signal. Transduct. Target. Ther. 5, 53.

Zygulska A.L. and Pierzchalski P. (2022). Novel diagnostic biomarkers in colorectal cancer. Int. J. Mol. Sci. 23, 852.

Figure legends

Figure 1. **SM exhibited potent antineoplastic activities *in vitro*.** After SW48 and LoVo cells exposure to SM with the concentration range from 0 μM to 32 μM for different incubating times, MTT (A) and clone formation for 72h (B), flow cytometry for 24h (C), transwell for 12h (D) and wound scratch for 24h (E) assays were utilized to evaluate cell proliferation, apoptosis, invasion and migration *in vitro*. n=3 in each group; $^{*}P<0.05$ and $^{***}P<0.001$ compared with control group.

Figure 2. **SM impeded LoVo cell growth *in vivo*.** After BALB/c nude mice were injected with LoVo cells (2×10^{6} cells) subcutaneously and intragastrically administrated with SM (5 mg/kg/day or 10 mg/kg/day) from day 10 to day 24, body weight of nude mice (A), tumor volume (B) and weight at day 24 (C). IHC staining of Ki67 and TUNEL were implemented to analyze the anti-proliferative and pro-apoptotic properties of SM *in vivo*. Histogram represented the quantitative analysis of the number of Ki67-positive and TUNEL-positive cells (D). Micrograph of HE staining, IHC staining of Ki67 and TUNEL of CRC tissues (E; magnification = 50x). n=6 in each group; $^{**}P<0.01$ and $^{***}P<0.001$ compared with control group. 5MPK, 5 mg/kg/day; 10MPK, 10 mg/kg/day.

Figure 3. **SM mediated multiple signal pathways to suppress LoVo cell growth.** To explore signaling pathways underlying SM-mediated CRC cell death, RNA-seq was implemented to filtrate DEGs in SM-treated LoVo cells with volcano plot (A) and heatmap (B). The top 10 DEGs were validated using RT-qPCR (C). SM mediated multiple signal pathways were evaluated using GO and KEGG enrichment analysis (D). n=3 in each group; $^{*}P<0.05$, $^{**}P<0.01$ and $^{***}P<0.001$ compared with control group.

Figure 4. **SM activates PTEN and inhibits PI3K/AKT signaling.** In order to investigate the impact of SM (32 μM) on PTEN and PI3K/AKT signaling *in vitro* after 48h incubation, western blot analysis was conducted for PTNE, AKT, p-AKT, and p-mTOR (A), while IF staining was performed for PTNE (B). Furthermore, to assess the effect of SM on PTEN and PI3K/AKT signaling *in vivo*, western blot analysis was carried out for PTNE, AKT, p-AKT, and p-mTOR (C), and IHC staining was conducted for p-AKT, PTNE and p-mTOR (D; bar = 25μm). n=3 in each group; $^{**}P<0.01$ and $^{***}P<0.001$ compared with control group; ns, no significant.

Figure 5. **PI3K/AKT agonist reverses SM-induced antineoplastic activities *in vitro***.
After LoVo cells were co-incubated with IGF-1 (100 ng/mL) and SM (32 μM) for 48h, cell proliferation, invasion and migration were evaluated using clone formation (A), transwell (B) and wound scratch (C), respectively. n=3 in each group; $^{*}P<0.05$, $^{**}P<0.01$ and $^{***}P<0.001$ compared with corresponding group.

Figure 6. **SM inhibits cell cycle and apoptosis signaling pathway.** After LoVo cells exposure to SM (32 μM) for 48h, western blot was used to measure PCNA and Cyclin E protein expression *in vitro* (A), and the protein expression of PCNA and Cyclin E was detected with western blot *in vivo* (B). In addition, apoptosis-related proteins were also measured by western blot *in vitro* after LoVo cells exposure to SM (32 μM) for 48h (C) and *in vivo* (D). IF staining and IHC staining were conducted for detecting BAX in LoVo cells (**E**) and tumor tissues (**F**) of transplanted tumor mice with SM treatment, respectively. n=3 in each group; $^{*}P<0.05$, $^{**}P<0.01$ and $^{***}P<0.001$ compared with control group; ns, not significant.

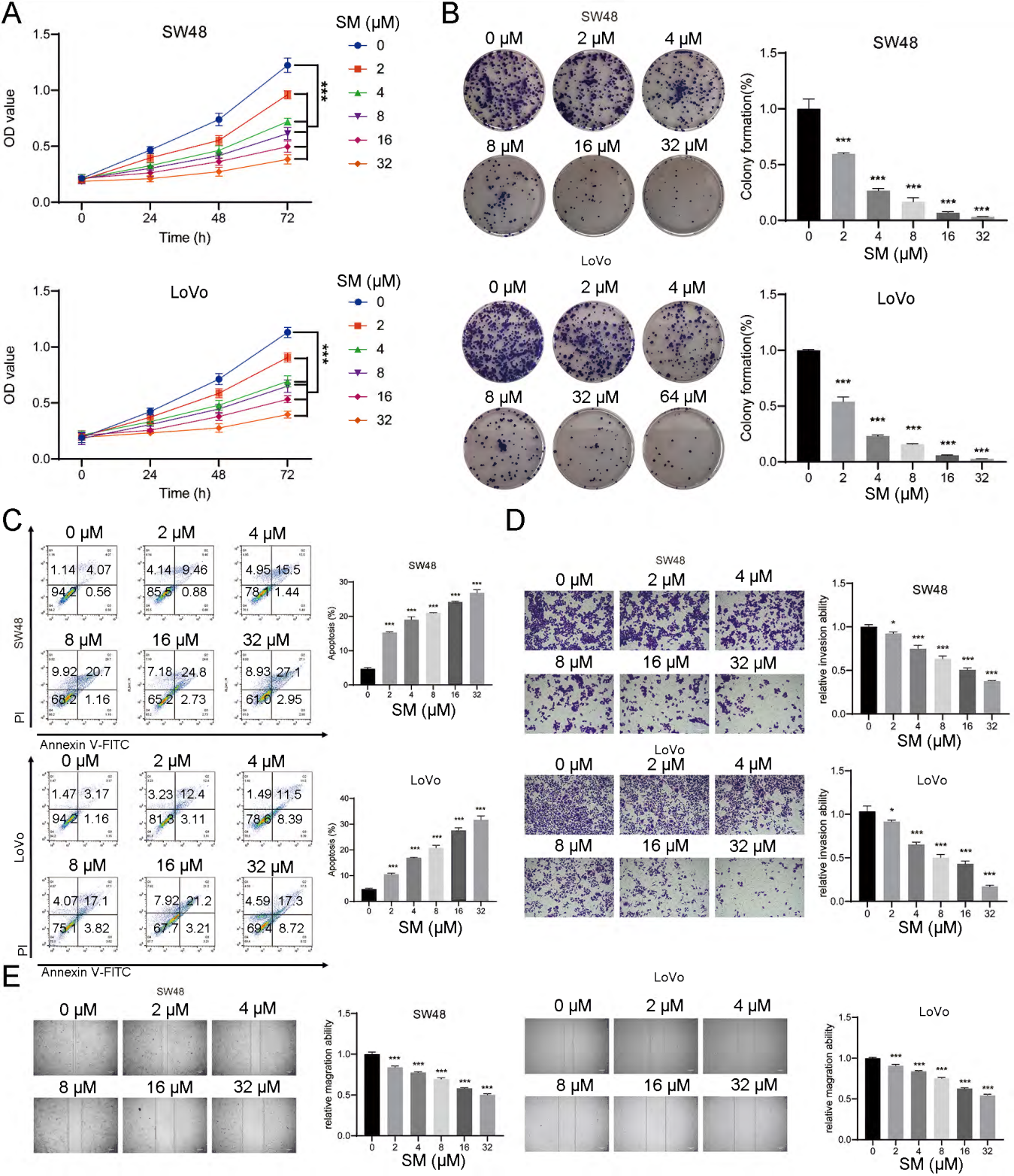
A
SW48
OD value
Time (h)
SM (μM)
0
2
4
8
16
32
***
LoVo
B
SW48
0 μM
2 μM
4 μM
8 μM
16 μM
32 μM
Colony formation(%)
SM (μM)
LoVo
64 μM
C
SW48
LoVo
PI
Annexin V-FITC
Apoptosis (%)
D
relative invasion ability
E
relative magration ability

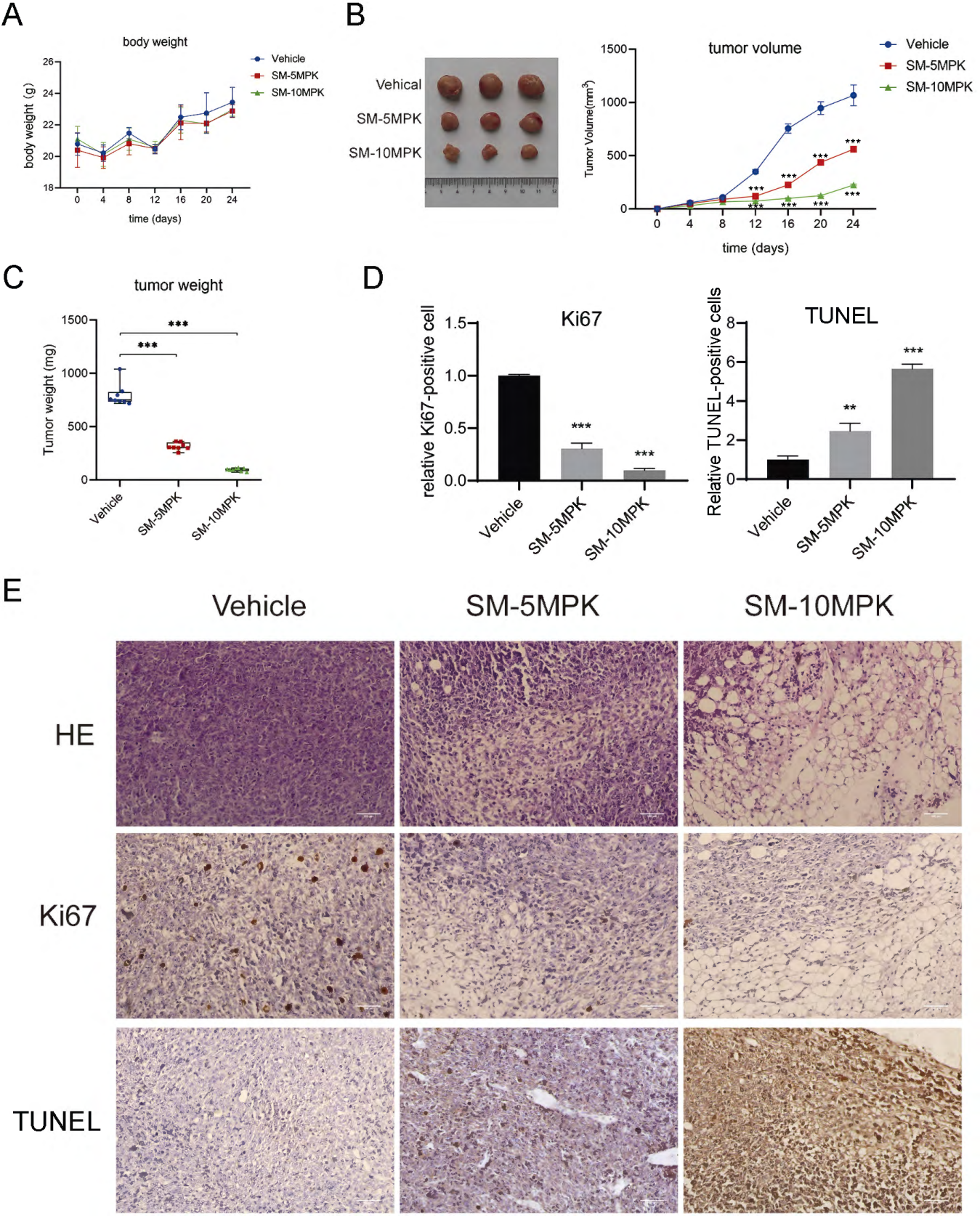
A
body weight
Vehicle
SM-5MPK
SM-10MPK
body weight (g)
time (days)
B
Vehical
SM-5MPK
SM-10MPK
tumor volume
Tumor Volume(mm3)
time (days)
C
tumor weight
Tumor weight (mg)
Vehicle
SM-5MPK
SM-10MPK
D
Ki67
relative Ki67-positive cell
TUNEL
Relative TUNEL-positive cells
E
Vehicle
SM-5MPK
SM-10MPK
HE
Ki67
TUNEL

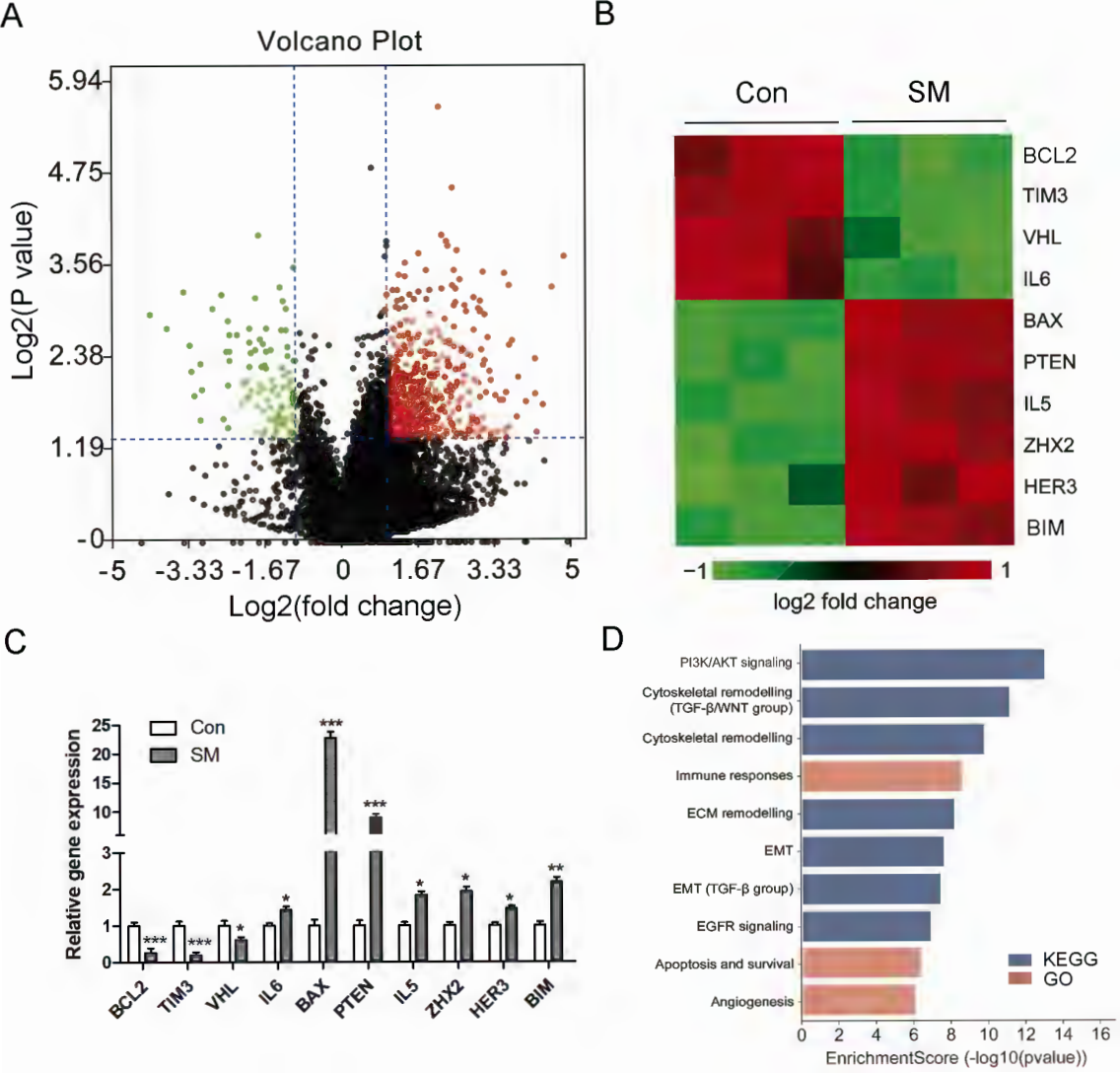
A
Volcano Plot
5.94
4.75
3.56
2.38
1.19
-0
Log2(P value)
-5
-3.33
-1.67
0
1.67
3.33
5
Log2(fold change)
B
Con
SM
BCL2
TIM3
VHL
IL6
BAX
PTEN
IL5
ZHX2
HER3
BIM
−1
1
log2 fold change
C
Relative gene expression
Con
SM
BCL2
TIM3
VHL
IL6
BAX
PTEN
IL5
ZHX2
HER3
BIM
D
PI3K/AKT signaling
Cytoskeletal remodelling (TGF-β/WNT group)
Cytoskeletal remodelling
Immune responses
ECM remodelling
EMT
EMT (TGF-β group)
EGFR signaling
Apoptosis and survival
Angiogenesis
KEGG
GO
EnrichmentScore (-log10(pvalue))

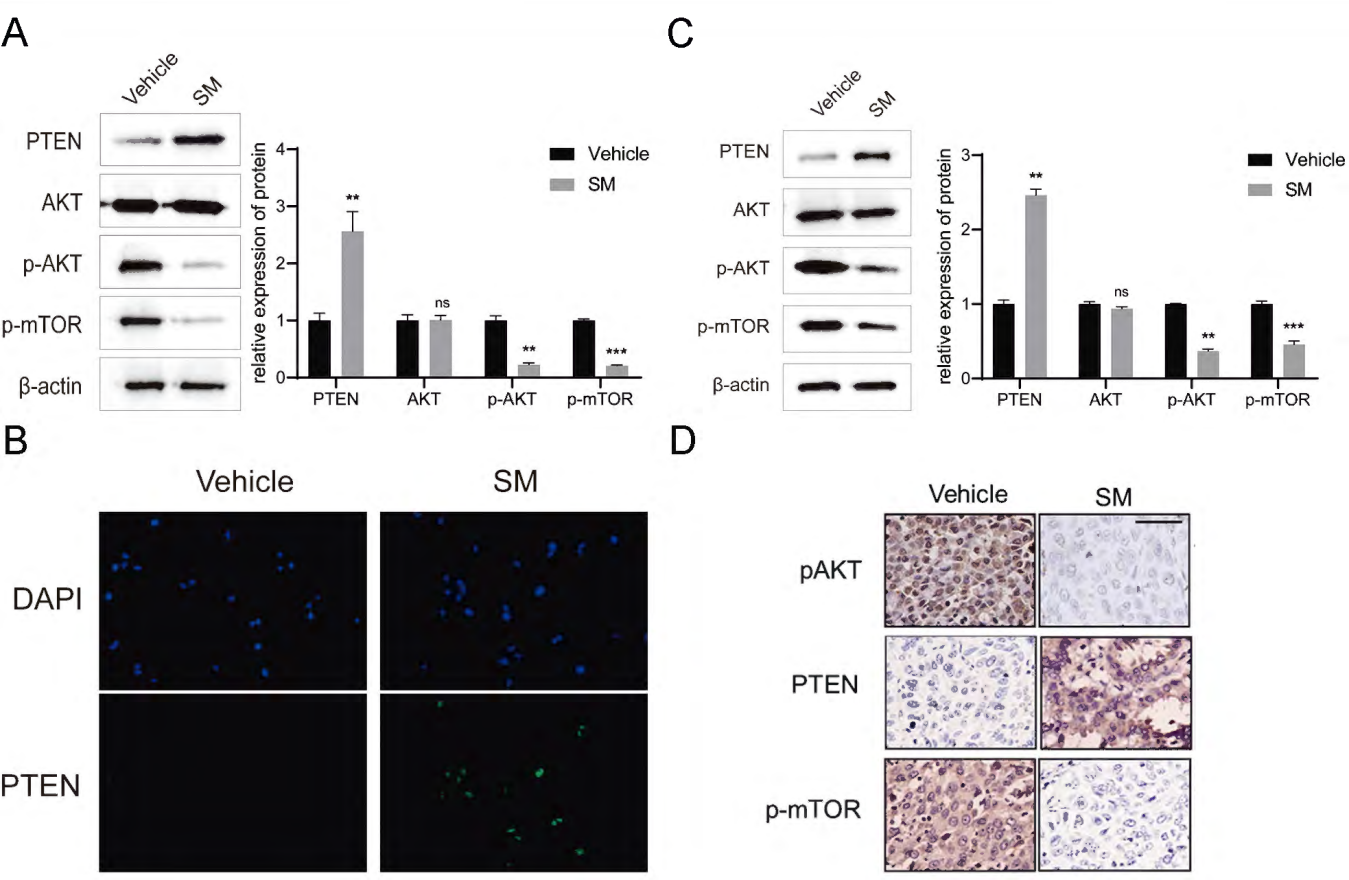
A
Vehicle
SM
PTEN
AKT
p-AKT
p-mTOR
β-actin
relative expression of protein
Vehicle
SM
**
ns
**
***
PTEN
AKT
p-AKT
p-mTOR
C
Vehicle
SM
PTEN
AKT
p-AKT
p-mTOR
β-actin
relative expression of protein
Vehicle
SM
**
ns
**
***
PTEN
AKT
p-AKT
p-mTOR
B
Vehicle
SM
DAPI
PTEN
D
Vehicle
SM
pAKT
PTEN
p-mTOR

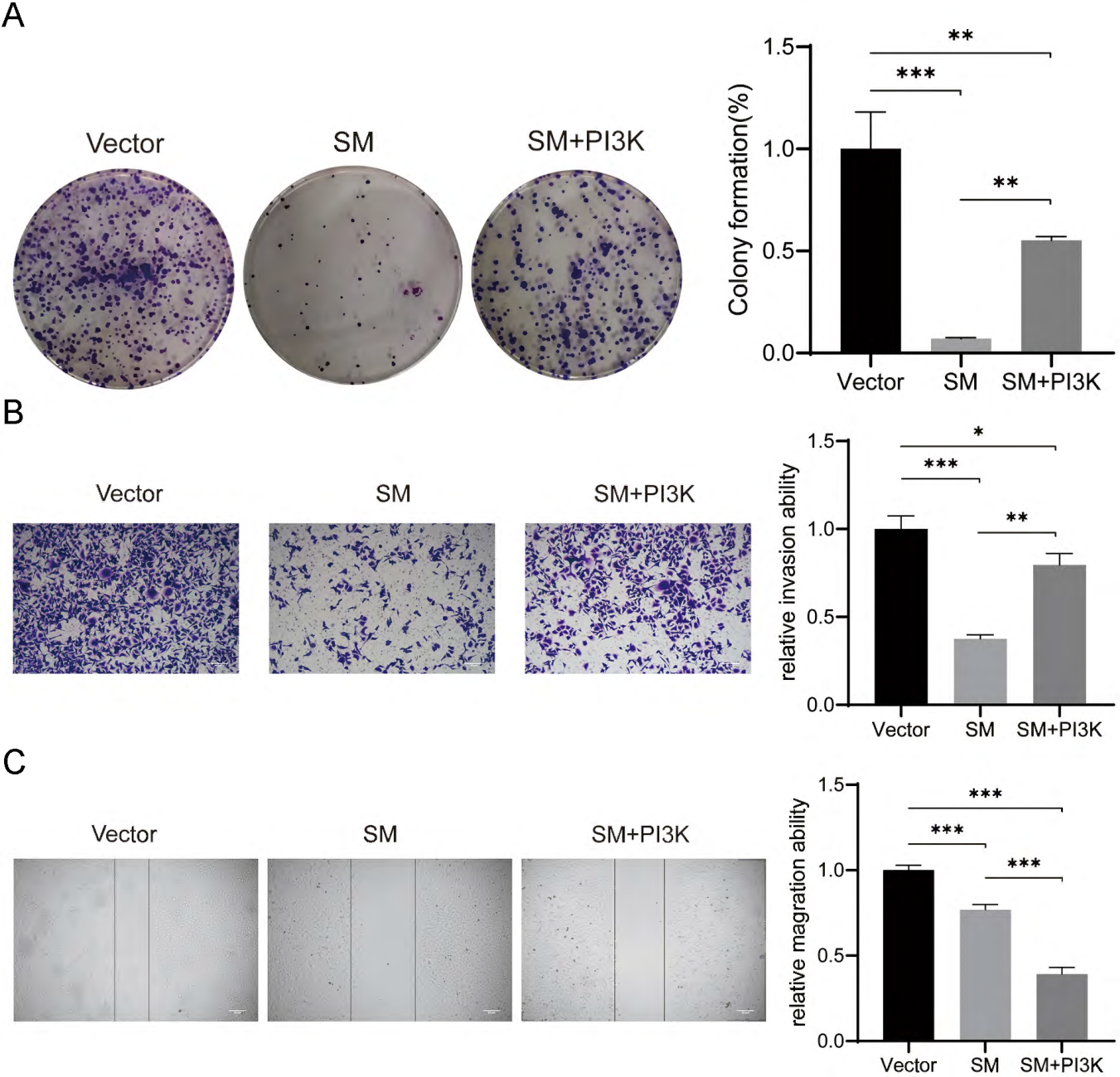
A
Vector
SM
SM+PI3K
Colony formation(%)
1.5
1.0
0.5
0.0
**
***
**
Vector
SM
SM+PI3K
B
Vector
SM
SM+PI3K
relative invasion ability
1.5
1.0
0.5
0.0
*
***
**
Vector
SM
SM+PI3K
C
Vector
SM
SM+PI3K
relative magration ability
1.5
1.0
0.5
0.0
***
***
***
Vector
SM
SM+PI3K

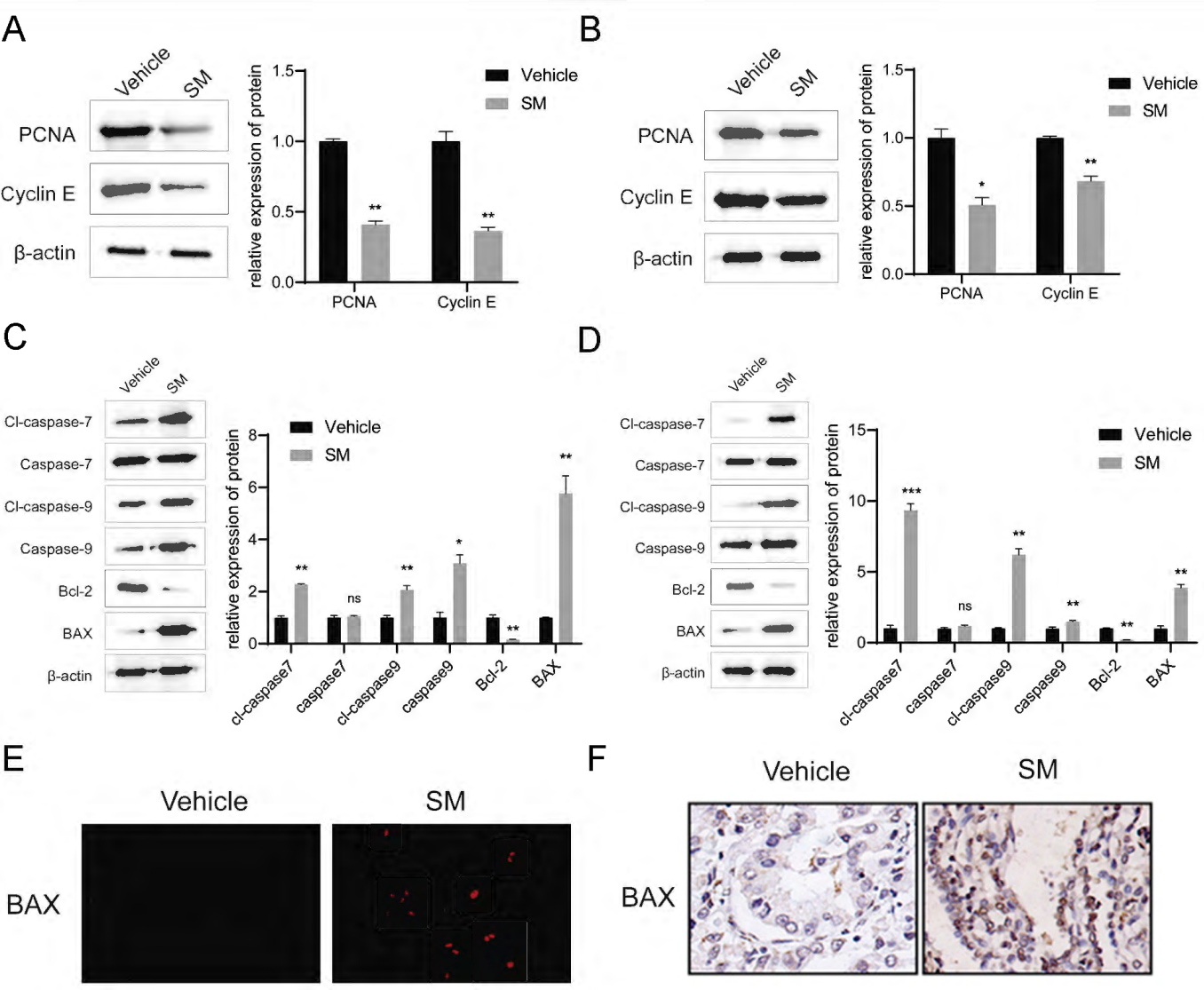
A
Vehicle
SM
PCNA
Cyclin E
β-actin
relative expression of protein
1.5
1.0
0.5
0.0
Vehicle
SM
**
**
PCNA
Cyclin E
B
Vehicle
SM
PCNA
Cyclin E
β-actin
relative expression of protein
1.5
1.0
0.5
0.0
Vehicle
SM
*
**
PCNA
Cyclin E
C
Vehicle
SM
Cl-caspase-7
Caspase-7
Cl-caspase-9
Caspase-9
Bcl-2
BAX
β-actin
relative expression of protein
8
6
4
2
0
Vehicle
SM
**
ns
**
*
**
**
cl-caspase7
caspase7
cl-caspase9
caspase9
Bcl-2
BAX
D
Vehicle
SM
Cl-caspase-7
Caspase-7
Cl-caspase-9
Caspase-9
Bcl-2
BAX
β-actin
relative expression of protein
15
10
5
0
Vehicle
SM
***
ns
**
**
**
**
cl-caspase7
caspase7
cl-caspase9
caspase9
Bcl-2
BAX
E
Vehicle
SM
BAX
F
Vehicle
SM
BAX